Tricarbonylbis(phosphine)iron(I) Cation Radicals. A Spectroscopic and Theoretical Study

Michael J. Therien and William C. Trogler*

Contribution from the Department of Chemistry, D-006, University of California at San Diego, La Jolla, California 92093. *Received November 14, 1985*

Abstract: Comparison of the IR spectra of $Fe(CO)_3(PPh_3)_2$ and the 17-electron complex $[Fe(CO)_3(PPh_3)_2][PF_6]$, each enriched 50% and 93% with ^{13}CO, shows that the 17-electron d^7 radical retains the trigonal-bipyramidal structure (D_{3h} coordination symmetry) of the parent complex. The IR and EPR spectra of other $Fe(CO)_3L_2^+$ (L = PMe_3, $P(n\text{-}Bu)_3$, $P(c\text{-}C_6H_{11})_3$) complexes are similar to that of $Fe(CO)_3(PPh_3)_2^+$ with ν_{CO} = 1974-1999 cm^{-1} and $\langle g \rangle$ = 2.053-2.057 (A_p = 17.5-18.7 G). SCF-Xα-DV calculations for the model complex $Fe(CO)_3(PH_3)_2^+$ of D_{3h} symmetry show a ground-state electronic configuration of $3e''^4$ ($d_{xz,yz}$) $6e'^3$ ($d_{x^2-y^2,xy}$). The $3e'' \rightarrow 6e'$ "d-d" transition was calculated to occur at 1.06 eV in the near-IR spectral region and was found at 1.16 eV in the electronic absorption spectrum of $[Fe(CO)_3(PCy_3)_2][PF_6]$. An absorption at 1.89 eV in the spectrum of the latter complex is assigned to the dipole-allowed $5a_1' \rightarrow 6e'$ transition, where $5a_1'$ is the Fe-P σ-bonding orbital. Calculations for assumed C_{2v} and C_s square-pyramidal isomers of $Fe(CO)_3(PH_3)_2^+$ did not agree with the electronic absorption spectrum of $[Fe(CO)_3(PCy_3)_2][PF_6]$.

Species other than 16- and 18-electron intermediates play important kinetic roles in organometallic reactions.[1-19] Most organotransition-metal carbonyl radicals studied to date are nonpersistent. Routes to generating these species include the irradiation and thermolysis of metal-metal-bonded dinuclear complexes,[8,11,13-15] 1-electron oxidation or reduction of 18- or 16-electron compounds by chemical[9,10,18-20] or electrochemical[3-7,16,17,19] means, and radical chain initiation.[1,11,12]

Table I. Infrared and Electron Paramagnetic Resonance Spectral Data for $Fe(CO)_3L_2^+$ Complexes[a]

compd	18e, ν_{CO}, cm^{-1}	17e, ν_{CO}, cm^{-1}	$\langle g \rangle$	$\langle A_P \rangle$[b]
$Fe(CO)_3(PPh_3)_2^{0/+}$	1878	1999	2.053	18.7[c]
$Fe(^{13}CO)_3(PPh_3)_2^{0/+}$	1839	1955	2.053	18.9[c]
$Fe(CO)_3(PCy_3)_2^{0/+}$	1846	1974	2.055	17.5[c]
$Fe(CO)_3(P(n\text{-}Bu)_3)_2^{0/+}$	1855	1980	2.057	18.5[d]
$Fe(CO)_3(PMe_3)_2^{0/+}$	1863	1990	2.056	18.2[d,e]

[a] All spectra taken in CH_2Cl_2 solvent. [b] Three lines with relative intensities of 1:2:1, in units of gauss. [c] Seventeen electron compounds isolated prior to spectral analysis. [d] Chemically generated in solution using the oxidant $[(4\text{-}BrC_6H_5)_3N][PF_6]$. [e] Unstable species, persists at 0 °C for short periods of time.

Because many organometallic carbonyl radicals are short lived, there is little structural and spectroscopic information available about them. Of the homoleptic transition-metal carbonyl radicals, only for the stable complex $V(CO)_6$ are electronic[21] and geometrical[22] structures well defined. Spectroscopic information and crystallographic data are lacking for homoleptic carbonyl radicals of chromium and iron.[20,23,24] Spectroscopic investigations have been limited[25] for even the well-studied $Mn(CO)_5$ radical and its phosphine-substituted derivatives, although EPR and IR spectra of $Mn(CO)_5$ trapped in several matrices[25] and IR and EPR data for $Mn(CO)_3(PR_3)_2$ complexes[14] have been taken as evidence for a square-pyramidal geometry. In contrast to the d^7 Mn radicals, EPR and IR spectroscopic data for several $Fe(CO)_3L_2^+$ complexes have been interpreted[20] in the context of a trigonal-bipyramidal structure.

Transition-metal pentacoordination has been a subject of theoretical interest.[26] Extended Hückel calculations[26a] suggest

(1) (a) Brown, T. L. *Ann. N. Y. Acad. Sci.* **1980**, *333*, 80-89. (b) Kochi, J. K. *Organometallic Mechanisms and Catalysis*; Academic: New York, 1978. (c) Collman, J. P.; Hegedus, L. S. *Principles and Applications of Organotransition Metal Chemistry*; University Science Books: Mill Valley, CA, 1980. (d) Lappert, M. F.; Lendor, P. W. *Adv. Organomet. Chem.* **1976**, *14*, 345-399.

(2) Darchen, A.; Mahé, C.; Patin, H. *J. Chem. Soc., Chem. Commun.* **1982**, 243-244.

(3) Hershberger, J. W.; Kochi, J. K. *J. Chem. Soc., Chem. Commun.* **1982**, 212-214.

(4) Hershberger, J. W.; Klinger, R. J.; Kochi, J. K. *J. Am. Chem. Soc.* **1982**, *104*, 3034-3043.

(5) Zizelman, P. M.; Amatore, C.; Kochi, J. K. *J. Am. Chem. Soc.* **1984**, *106*, 3771-3790.

(6) Magnuson, R. H.; Zulu, S.; T'sai, W.-M.; Giering, W. P. *J. Am. Chem. Soc.* **1980**, *102*, 6887-6888.

(7) Magnuson, R. H.; Meriowitz, R.; Zulu, S.; Giering, W. P. *J. Am. Chem. Soc.* **1982**, *104*, 5790-5791.

(8) (a) Stiegman, A. E.; Goldman, A. S.; Leslie, D. B.; Tyler, D. R. *J. Chem. Soc., Chem. Commun.* **1984**, 632-633. (b) Stiegman, A. E.; Stieglitz, M.; Tyler, D. R. *J. Am. Chem. Soc.* **1983**, *105*, 6032-6037. (c) Goldman, A. S.; Tyler, D. R. *J. Am. Chem. Soc.* **1984**, *106*, 4066-4067. (d) Stiegman, A. E.; Tyler, D. R. *Inorg. Chem.* **1984**, *23*, 527-529.

(9) Shi, Q.-Z.; Richmond, T. G.; Trogler, W. C.; Basolo, F. *J. Am. Chem. Soc.* **1982**, *104*, 71-76.

(10) Richmond, T. G.; Shi, Q.-Z.; Trogler, W. C.; Basolo, F. *J. Am. Chem. Soc.* **1982**, *104*, 76-80.

(11) (a) Okuhara, K. *J. Am. Chem. Soc.* **1980**, *102*, 244-252. (b) Lawrence, L. M.; Whitesides, G. M. *J. Am. Chem. Soc.* **1980**, *102*, 2493-2494. (c) Ashby, E. C.; Bowers, J. R., Jr. *J. Am. Chem. Soc.* **1981**, *103*, 2242-2250. (d) Poë, A.; Sekbar, C. V. *J. Am. Chem. Soc.* **1985**, *107*, 4874-4883.

(12) Wegman, R. W.; Brown, T. L. *Organometallics* **1982**, *1*, 47-52.

(13) (a) Kidd, D. R.; Brown, T. L. *J. Am. Chem. Soc.* **1978**, *100*, 4095-4103. (b) Byers, B. H.; Brown, T. L. *J. Am. Chem. Soc.* **1977**, *99*, 2527-2532. (c) Absi-Halabi, M.; Brown, T. L. *J. Am. Chem. Soc.* **1977**, *99*, 2982-2988. (d) Wegman, R. W.; Olson, R. J.; Gard, D. R.; Faulkner, L. R.; Brown, T. L. *J. Am. Chem. Soc.* **1981**, *103*, 6089-6092. (e) Herrinton, T. R.; Brown, T. L. *J. Am. Chem. Soc.* **1985**, *107*, 5700-5703.

(14) (a) McCullen, S. B.; Brown, T. L. *J. Am. Chem. Soc.* **1982**, *104*, 7496-7500. (b) McCullen, S. B.; Walker, H. W.; Brown, T. L. *J. Am. Chem. Soc.* **1982**, *104*, 4007-4008. (c) Rattinger, G.; Belford, R. L.; McCullen, S. B.; Walker, H. W.; Brown, T. L., results cited in ref 14a.

(15) (a) Wrighton, M. S.; Ginley, D. S. *J. Am. Chem. Soc.* **1975**, *97*, 2065-2072. (b) Hepp, A. F.; Wrighton, M. S. *J. Am. Chem. Soc.* **1983**, *105*, 5935-5937. (c) Hepp, A. F.; Wrighton, M. S. *J. Am. Chem. Soc.* **1981**, *103*, 1258-1261.

(16) Doxsee, K. M.; Grubbs, R. H.; Anson, F. C. *J. Am. Chem. Soc.* **1984**, *106*, 7819-7824.

(17) Narayanan, B. A.; Kochi, J. K. *J. Organomet. Chem.* **1984**, *272*, C49-C53.

(18) Krusic, P. J.; Briere, R.; Rey, P. *Organometallics* **1985**, *4*, 801-803.

(19) Therien, M. J.; Ni, C. L.; Anson, F. C.; Osteryoung, J. G.; Trogler, W. C. *J. Am. Chem. Soc.*, in press.

(20) Baker, P. K.; Connelly, N. G.; Jones, B. M. R.; Maher, J. P.; Somers, K. R. *J. Chem. Soc., Dalton Trans.* **1980**, 579-584.

(21) Holland, G. F.; Manning, M. C.; Ellis, D. E.; Trogler, W. C. *J. Am. Chem. Soc.* **1983**, *105*, 2308-2314.

(22) (a) Wilson, R. D.; Bau, R. J. *J. Am. Chem. Soc.* **1974**, *96*, 7601-7602. (b) Bellard, S.; Rubinson, K. A.; Sheldrick, G. M. *Acta Crystallogr., Sect. B.* **1979**, *35*, 271-274.

(23) (a) Fairhurst, S. A.; Morton, J. R.; Preston, K. F. *J. Chem. Phys.* **1982**, *77*, 5872-5875. (b) Lionel, T.; Morton, J. R.; Preston, K. F. *J. Chem. Phys.* **1982**, *76*, 234-239.

(24) Peake, B. M.; Symons, M. C. R.; Wyatt, J. L. *J. Chem. Soc., Dalton Trans.* **1983**, *1171*-1174.

(25) (a) Howard, J. A.; Morton, J. R.; Preston, K. F. *Chem. Phys. Lett.* **1981**, *2*, 226-228. (b) Lionel, T.; Morton, J. R.; Preston, K. F. *Chem. Phys. Lett.* **1981**, *1*, 17-20. (c) Church, S. P.; Poliakoff, M.; Timney, J. A.; Turner, J. J. *J. Am. Chem. Soc.* **1981**, *103*, 7515-7520. (d) Fairhurst, S. A.; Morton, J. R.; Perutz, R. N.; Preston, K. F. *Organometallics* **1984**, *3*, 1389-1391. (e) Symons, M. C. R.; Sweany, R. L. *Organometallics* **1982**, *1*, 834-836.

0002-7863/86/1508-3697$01.50/0

that trigonal-bipyramidal and square-pyramidal geometries are energetically comparable for pentacoordinate d^7 metal radicals. It is known that the low-spin d^7 Co(II) complexes $Co(dpe)_2Cl^+$ adopt both square-pyramidal and trigonal-bipyramidal structures in the solid state.[27]

In this paper we report EPR and optical spectroscopic data, IR spectroscopic studies of ^{13}C-labeled complexes, and electronic structure calculations using the SCF-Xa-DV method,[28] which support a trigonal-bipyramidal (D_{3h}) ground-state structure for tricarbonylbis(phosphine)iron(I) cation radicals. We show that the statistical ^{13}C-labeling technique can be used to determine the solution-state structure of a d^7 ML_5 radical just as has been done for matrix-isolated species. The trigonal-bipyramidal geometry established here for $Fe(CO)_3L_2^+$ contrasts with isoelectronic $Mn(CO)_{5-n}L_n$ ($n \leq 2$; L = phosphine) species, which are believed to have a ground-state geometry derived from C_{4v} symmetry.

Results and Discussion

Spectral Studies. The presence of a single absorption in the IR spectrum of $Fe(CO)_3(PPh_3)_2^+$, in addition to a triplet hyperfine splitting pattern in the EPR spectrum, was taken by Baker et al.[20] to establish a D_{3h} structure for this and related iron(I) radicals. Conclusive proof of structures for these fundamental systems is needed. We examined a series of bis(phosphine)-substituted $Fe(CO)_3L_2^+$ compounds (Table I) that gives EPR and IR spectra data in good agreement to that previously reported[20] and extends the series to bulky (PCy_3) and small (PMe_3) phosphine ligands. Infrared spectra show a single absorption in the carbonyl region for each of the 17-electron $Fe(CO)_3L_2^+$ complexes regardless of the phosphine ligand's size. All compounds exhibit three-line EPR spectra with intensities of 1:2:1, consistent with coupling of the unpaired electron to two equivalent phosphorus atoms in a static D_{3h}, C_{2v}, or C_s structure or in a fluxional C_s square-pyramidal structure. Low-temperature (77 K) spectra of $Fe(CO)_3(PCy_3)_2^+$ and $Fe(CO)_3(PPh_3)_2^+$ resemble those at room temperature and show little anisotropy (using the SIM14 program[29] to reproduce the spectra) in the g tensor.

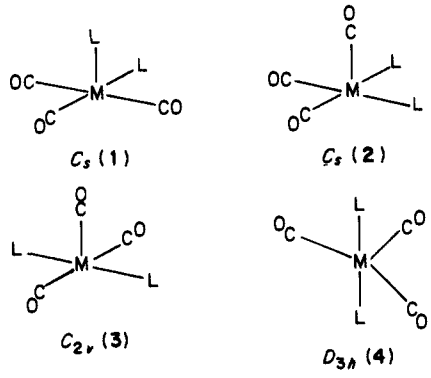

Significant differences exist among the reported EPR data for iron pentacarbonyl cation radicals. Spectra of $Fe(CO)_5^+$ doped in a single crystal of $Cr(CO)_6$[23b] show that the species produced has C_{4v} symmetry with $g_{av} = 2.055$; however, for $Fe(CO)_5^+$ generated in trichlorofluoromethane[24] $g_{av} = 2.039$. Solution EPR spectra (Table I) of substituted iron carbonyl cation radicals studied here and by other investigators[20,30] yield values of g_{av} between 2.030 and 2.060. These data raise several questions: (1) EPR spectra taken of metal radicals doped in single crystals may not be representative of the same species present in solution. For example, the $Cr(CO)_6$ host lattice may induce a C_{4v} geometry (i.e., octahedrally derived) in the trapped $Fe(CO)_5^+$ radical. (2) Measured g_{av} values of $Fe(CO)_{5-n}L_n^+$ species seem to be sensitive to the steric and electronic nature of the ligand L. It seems tenuous, at best, to assign a ground-state structure to d^7 metal radical species based on EPR evidence alone. This problem has also been recognized[27] for d^7 Co(II) complexes.

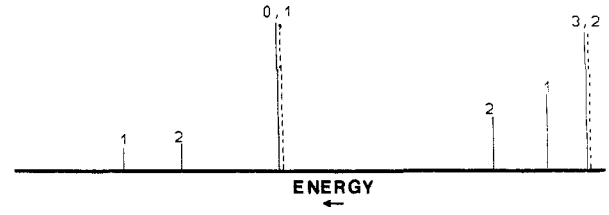

Figure 1. Expected relative intensity and proximity of carbonyl stretching absorptions depicted for a 50% ^{13}CO-labeled D_{3h} $M(CO)_3(PR_3)_2$ complex calculated for a principal to interaction force constant ratio of 100 (R = 100). The labels correspond to the following species: 0 = $M(CO)_3(PR_3)_2$, 1 = $M(^{13}CO)(CO)_2(PR_3)_2$, 2 = $M(^{13}CO)_2(CO)(PR_3)_2$, 3 = $M(^{13}CO)_3(PR_3)_2$. This figure was adopted from calculations in ref 31a.

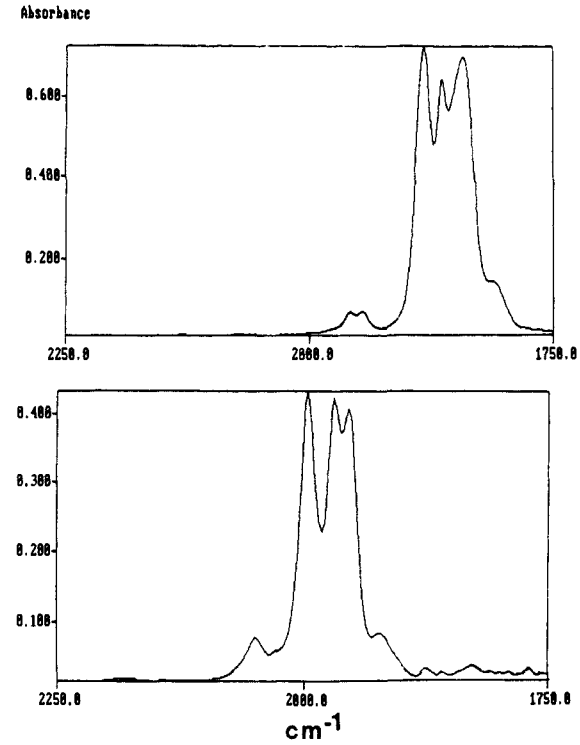

Figure 2. (A, top) Infrared absorptions of 50% ^{13}CO-labeled $Fe(CO)_3(PPh_3)_2$. (B, bottom) Infrared absorptions of the similarly labeled 17-electron complex, $Fe(CO)_3(PPh_3)_2^+$. IR spectra were recorded in CH_2Cl_2 solvent at 22 °C.

^{13}CO-Labeling Studies. The single CO absorption in the IR spectra of $Fe(CO)_3L_2^+$ complexes could arise from a D_{3h} static structure or from accidental overlap of more than one CO absorption from a square-pyramidal structure. The presence of two equivalent phosphines in the EPR (even at 77 K) spectrum argues against structure **1**. Attempts to crystallize the radicals failed because of instability of these solutions to disproportionation.[19] To gain further information about the soluton structure of $Fe(CO)_3L_2^+$ complexes, a ^{13}CO-labeling study was undertaken. A diagrammatic representation of the infrared spectrum expected[31a]

(26) (a) Rossi, A. R.; Hoffmann, R. *Inorg. Chem.* **1975**, *14*, 365–374. (b) Burdett, J. K. *Inorg. Chem.* **1975**, *14*, 375–382. (c) Holmes, R. R. In *Progress in Inorganic Chemistry*; Lippard, S. J., Ed.; Wiley: New York, 1984; Vol. 32, pp 119–237.

(27) Stalick, J. K.; Corfield, P. W. R.; Meek, D. W. *Inorg. Chem.* **1973**, *12*, 1668–1675.

(28) (a) Ellis, D. E.; Painter, G. S. *Phys. Rev. B: Solid State* **1970**, *2*, 2887–2898. (b) Delley, B.; Ellis, D. E. *J. Chem. Phys.* **1982**, *76*, 1949–1960.

(29) Lozos, G. P.; Hoffman, B. M.; Franz, C. G. *QCPE* **1974**, *11*, 265.

(30) Krusic, P. J. Presented at the 190th National Meeting of the American Chemical Society, Sept 1985; INOR 0263.

(31) (a) Darling, J. H.; Ogden, J. S. *J. Chem. Soc., Dalton Trans.* **1972**, 2496–2503. (b) Haas, H.; Sheline, R. K. *J. Chem. Phys.* **1967**, *47*, 2996–3021. (c) Bor, G. *J. Organomet. Chem.* **1967**, *10*, 343–359. (d) Perutz, R. N.; Turner, J. J. *Inorg. Chem.* **1975**, *14*, 262–270 and references therein. (e) Burdett, J. K.; Dubost, H.; Poliakoff, M.; Turner, J. J. In *Advances in Infrared and Raman Spectroscopy*; Clark, R. J. H.; Hester, R. E., Eds.; Heyden: London, 1976; Vol. 2, pp 1–52.

Table II. Energies of IR-Allowed Vibrations for $Fe(CO)_3(PPh_3)_2^{0/+}$, $Fe(^{13}CO)(CO)_2(PPh_3)_2^{0/+}$, $Fe(^{13}CO)_2(CO)(PPh_3)_2^{0/+}$, and $Fe(^{13}CO)_3(PPh_3)_2^{0/+}$

complex	IR-allowed vibrational modes	18e, ν_{CO}, cm^{-1}	17e, ν_{CO}, cm^{-1}
$Fe(CO)_3(PPh_3)_2^{0/+}$	E′	1878	1999
$Fe(^{13}CO)(CO)_2(PPh_3)_2^{0/+}$	$1A_1$	1862[b]	1972[b]
	$2A_1$	1958	2049[b]
	B_2	1878	1999
$Fe(^{13}CO)_2(CO)(PPh_3)_2^{0/+}$	$1A_1$	1862[b]	1972[b]
	$2A_1$	1945	2049[b]
	B_2	1839	1955
$Fe(^{13}CO)_3(PPh_3)_2^{0/+}$	E′	1839	1955

[a] Values obtained from examination of the infrared spectra of unlabeled, 50% ^{13}CO-labeled, and 93% ^{13}CO-labeled $Fe(CO)_3(PPh_3)_2^{0/+}$ [b] Broad absorption caused by overlap of A_1 vibrations from singly and doubly ^{13}CO-labeled $Fe(CO)_3L_2^{0/+}$ species.

for a 50% ^{13}CO-labeled $M(CO)_3L_2$ compound (possessing D_{3h} symmetry) is shown in Figure 1. Note that a D_{3h} $M(CO)_3L_2$ molecule (one IR-active E′ mode) has its vibrational symmetry reduced to C_{2v} ($2A_1 + B_2$ IR-active vibrations) on isotopic substitution. For an excellent discussion of this technique and applications to structure determinations of metal carbonyls trapped in matrices, see ref 31a–e. A 50% ^{13}CO-labeled complex, which possessed a square-pyramidal geometry, would have more allowed CO stretching absorptions to yield a complex spectrum.

A 50% ^{13}CO-labeled sample of 18-electron $Fe(CO)_3(PPh_3)_2$ shows the IR spectrum (Figure 2A) expected for a D_{3h} coordination geometry. *Because $Fe(CO)_3L_2$ complexes have crystallography and spectroscopically determined*[32] *trigonal-bipyramidal geometries, the spectrum in Figure 2A can be taken as the fingerprint of a 50% ^{13}CO-labeled $M(CO)_3L_2$ complex of D_{3h} symmetry.* This spectrum resembles that calculated[31a] with a force constant ratio (the ratio of principal to interaction force constants) of 100 (Figure 1). The exact origin of the weak shoulder to low energy of the main band system is unknown. Its intensity remains unchanged even after recrystallization or column chromatographic purification. A reduction in ideal D_{3h} symmetry can arise from the presence of bulky phosphine ligands and produce weak features. In any event this absorption is taken as part of the fingerprint for the D_{3h} structure with axial PPh_3 ligands.

After the labeled compound was oxidized and $[Fe(^*CO)_3(PPh_3)_2][PF_6]$[20] was isolated, the IR spectrum of Figure 2B was obtained. Aside from a 100-cm^{-1} shift in vibrational frequencies (Table II), there are minor differences between the spectra of Figure 2 (overlap of the A_1 stretching modes of singly and doubly ^{13}CO-labeled $Fe(CO)_3L_2^+$ and a slight change in relative intensities of absorptions at lower energy). These differences may arise from a change in the force constant ratio. As electron density is removed from iron on oxidation, Fe–CO π bonding should decrease. This should alter electronic coupling through the π system and change the value of the interaction force constant. Since the cation is subject to a Jahn–Teller distortion (vide infra), slight differences in intensities and positions of the CO absorptions may occur. The striking similarity between the IR spectra of the neutral and oxidized species provides compelling evidence that $Fe(CO)_3L_2^+$ radicals retain a ground-state structure close to the trigonal-bipyramidal geometry of the neutral complex.

Theoretical Studies. Metal radicals possess characteristic low-energy electronic transitions in solution[9,10,13-15] and in the solid state.[21] To better understand the origin of these transitions as well as obtain a quantitative picture of bonding, SCF–Xα–DV calculations were performed on the model compound, $Fe(CO)_3(PH_3)_2^+$, with both D_{3h} and C_{2v} (**3**) structures. The C_{2v} (**3**) structure is that proposed[14] for isoelectronic $Mn(CO)_3L_2$ radicals.

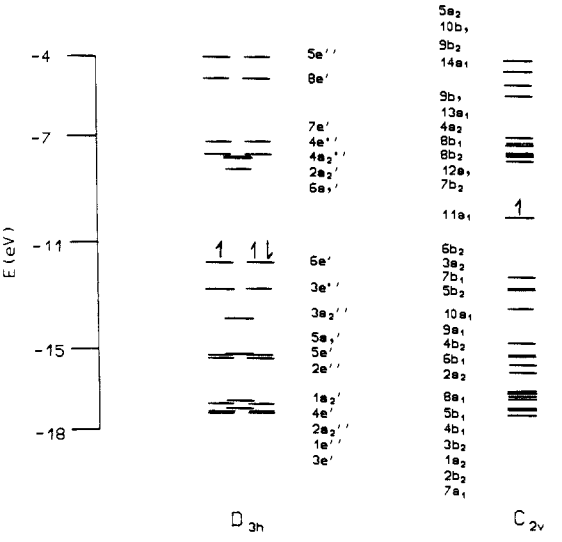

Figure 3. Orbital energy level diagram from SCF–Xα–DV calculations of $Fe(CO)_3(PH_3)_2^+$ with D_{3h} and C_{2v} (**3**) structures.

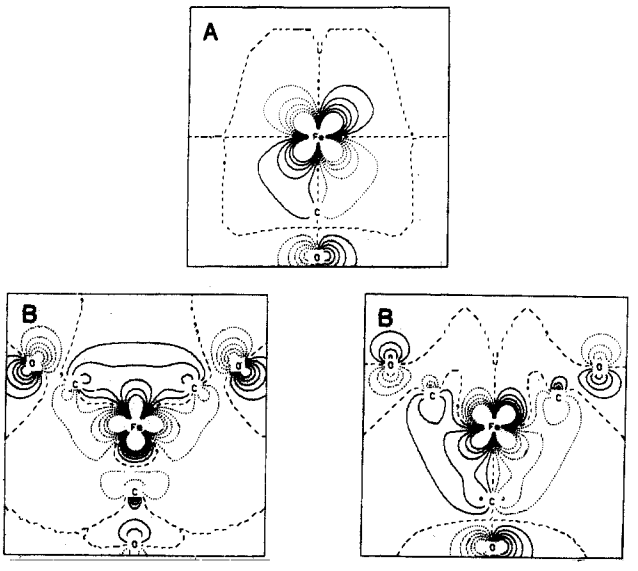

Figure 4. (A) Contour plot of a 3e″ orbital of D_{3h} $Fe(CO)_3(PH_3)_2^+$ in an $Fe(CO)(PPh_3)_2$ plane. The interval between successive contours is 0.270 e/Å^3. (B) Contour plot of the 6e′ orbitals of D_{3h} $Fe(CO)_3(PH_3)_2^+$ in an $Fe(CO)_3$ plane. The interval between successive contours is 0.270 e/Å^3. Both degenerate orbitals are shown.

Energy level diagrams for the frontier orbitals are shown in Figure 3 for spin-restricted calculations, while Table III gives orbital energies and their atomic character. Exchange energies from a spin-polarized calculation are also presented for the D_{3h} structure. From this table it is seen that only orbitals containing significant Fe 3d character show an appreciable exchange splitting. Calculated spin distributions and orbital populations for the valence orbitals in D_{3h} $Fe(CO)_3(PH_3)_2^+$ (Table IV) show that the odd electron primarily resides on the Fe atom.

Calculations predict the ground electronic state to be $^2E'$ for the D_{3h} structure and subject to Jahn–Teller distortion along the three e′ normal vibrational coordinates. There is no firm experimental evidence for the distortion. The nearly isotropic g factor suggests that quenching of electronic orbital angular momentum has occurred. As mentioned above, IR spectra perhaps show evidence for a slight distortion.

Except for 3e′ and $5a_1'$ the lower valence orbitals shown in Figure 3 for the D_{3h} structure are comprised mostly of ligand character (Table IIIA). The 3e″ orbital (Figure 4A) shows some Fe–CO π bonding and is composed of metal d_{xz} character (z along C_3). The partially filled HOMO (Figure 4B), the 6e′ orbital, shows bonding between $d_{x^2-y^2,xy}$ and the CO π^* orbitals. Although this orbital contains a small amount (7%) of Fe 4p character, d–p

(32) (a) Cowley, A. H.; Davis, R. E.; Ramadna, K. *Inorg. Chem.* **1981**, *20*, 2146–2152. (b) Ginderow, D. *Acta Crystallogr.; Sect. B* **1974**, *30*, 2798. (c) Shriver, D. F.; Whitmire, K. H. In *Comprehensive Organometallic Chemistry*; Wilkinson, G., Stone, F. G. A., Abel, E. W., Eds.; Pergamon: Oxford, 1982; Vol. 4, pp 243–330.

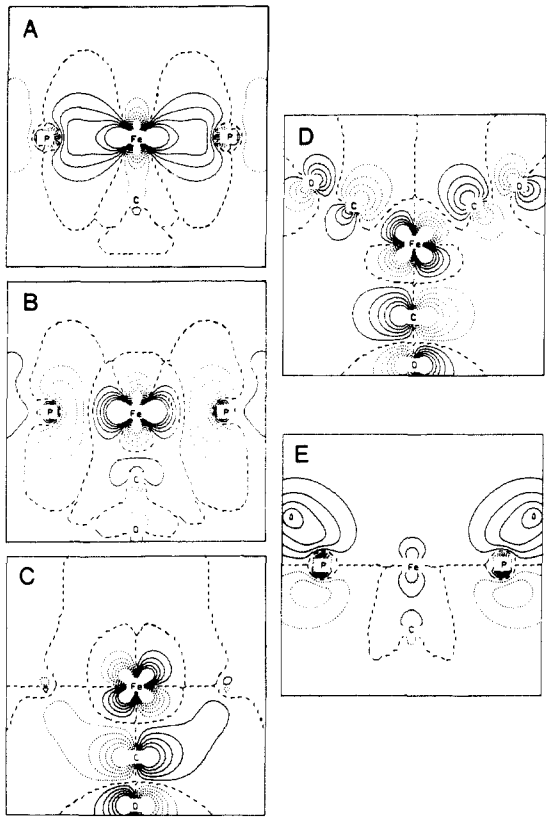

Figure 5. (A) Contour plot of the $5a_1'$ orbital of D_{3h} $Fe(CO)_3(PH_3)_2^+$ in an $Fe(CO)(PH_3)_2$ plane. The interval between successive contours is 0.270 e/Å^3. (B) Contour plot of the $6a_1'$ orbital of D_{3h} $Fe(CO)_3(PH_3)_2^+$ in an $Fe(CO)(PH_3)_2$ plane. The interval between successive contours is 0.270 e/Å^3. (C) Contour plot of a 4e″ orbital of D_{3h} $Fe(CO)_3(PH_3)_2^+$ in an $Fe(CO)(PPh_3)_2$ plane. The interval between successive contours is 0.270 e/Å^3. (D) Contour plot of a 7e′ orbital of D_{3h} $Fe(CO)_3(PH_3)_2^+$ in an $Fe(CO)_3$ plane. The interval between successive contours is 0.270 e/Å^3. (E) Contour plot of a 5e′ orbital of D_{3h} $Fe(CO)_3(PH_3)_2^+$ in an $Fe(CO)_3$ plane. The interval between successive contours is 0.270 e/Å^3.

hybridization is not as extensive as thought previously on the basis[26a] of extended Hückel calculations. No ^{13}C hyperfine structure was observed in the EPR spectrum of 93% ^{13}CO-enriched $Fe(^*CO)_3(PPh_3)_2^+$; however, this is consistent with the calculated spin distribution (Table IV). Contour plots of four other orbitals that contain significant metal character ($5a_1'$, $6a_1'$, 4e″, and 7e′) are shown in Figure 5, parts A–D. A contour plot of 5e′, an orbital that will be considered in the transition-state caculations, is also depicted in Figure 5E.

Transition-state calculations (Table V) provided energies of electronic transitions in both C_{2v} and D_{3h} $Fe(CO)_3(PH_3)_2^+$. For the D_{3h} model only the six lowest energy spin and dipole-allowed electronic transitions were considered: 3e″ → 6e′, $5a_1'$ → 6e′, 5e′ → 6e′, 6e′ → $6a_1'$, 6e′ → 4e″, and 6e′ → 7e′. The first entry in Table VA shows good agreement between the calculated 3e″ → 6e′ ("d–d") electronic transition for D_{3h} $Fe(CO)_3(PH_3)_2^+$ and the experimental near-infrared absorption seen in the spectrum of $Fe(CO)_3(PCy_3)_2^+$ (only 0.1 eV separates experiment and theory). Absorptions in the UV region of the electronic spectrum correlate well with those predicted by theory: 5e′ → 6e′ (phosphine ligand to metal charge transfer), 6e′ → $6a_1'$ (metal to Fe–P σ^*), 6e′ → 4e″ (metal to CO ligand charge transfer), and 6e′ → 7e′ (metal to CO ligand charge transfer). Because the experimental charge-transfer absorptions overlap, other contributing electronic transitions from lower lying orbitals (i.e., 2e″, 4e′, etc.) were not considered in the calculations.

The only discrepancy between experiment and theory occurs for the transition at 1.89 eV, which imparts the intense green color to these complexes. Two transitions ($5a_1'$ → 6e′, 6e′ → $6a_1'$) that might be attributed to this absorption involve the $5a_1'$ and $6a_1'$ orbitals (Figure 5) that contain substantial phosphorus lone-pair

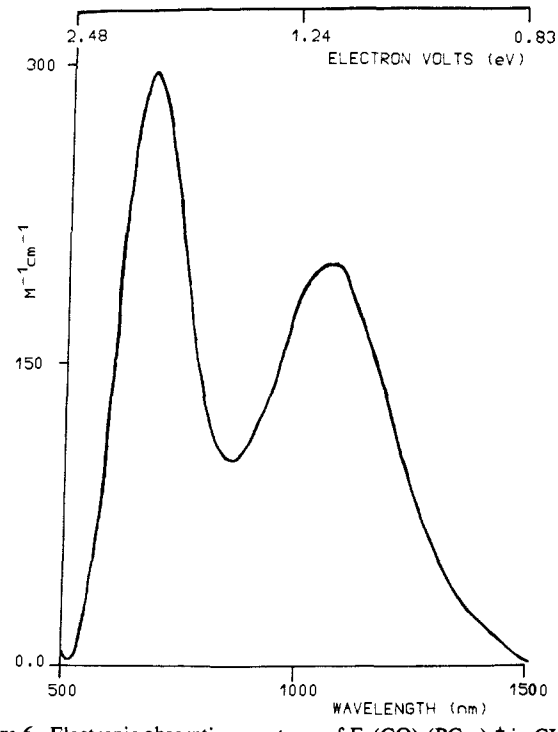

Figure 6. Electronic absorption spectrum of $Fe(CO)_3(PCy_3)_2^+$ in CH_2Cl_2 at 22 °C.

character. The quantitative disagreement between theory and experiment may be rationalized by considering energies of the frontier orbitals in phosphine (PH_3) and in trialkylphosphines (PR_3). Previous SCF-Xα-DV calculations[33] show that the HOMO (a_1 symmetry, P lone pair) of $P(CH_3)_3$ is raised in energy as compared to PH_3. This would cause the Fe–P σ-bonding orbital, $5a_1'$, to raise in energy and thereby lower the energy of the $5a_1'$ → 6e′ transition, which would better agree with the experimental absorption at 1.89 eV. Similar destabilization of $6a_1'$ should occur since it too contains P lone-pair character. This will shift the 6e′ → $6a_1'$ transition to higher energy (i.e., the charge-transfer region) where the experimental spectrum is complex.

As a further test of the D_{3h} structural assignment, we performed transition-state calculations (Table VB) for alternative square-pyramidal isomers (C_{2v} (**3**) and C_s (**2**)). The C_{2v} isomer, analogous to that proposed[14] for $Mn(CO)_3L_2$ radicals, exhibits frontier valence orbitals (Table IIIB) primarily localized on iron. They differ qualitatively from those of the D_{3h} isomer. Five of the eight lowest spin- and dipole-allowed transitions (Table V) occur at 2.51 ± 0.2 eV, and the calculated energies do not correlate well with the transitions observed for $Fe(CO)_3(PCy_3)_2^+$. Allowing for destabilization of phosphorus lone-pair orbitals in comparing the theoretical PH_3 complex to the PCy_3 derivative would red shift the $5b_2$ → $11a_1$ and $10a_1$ → $11a_1$ transitions and blue shift the $11a_1$ → $12a_1$ transition. Four of the five transitions centered near 2.5 eV would remain and should produce a more complex visible absorption spectrum than that observed. The frontier valence orbitals of the C_s (**2**) isomer are qualitatively similar to those of the C_{2v} species, and transition-state calculations predict an even worse correlation with the experimental absorption spectrum. Tables of orbital energies and transition-state calculations are available as supplementary material.

Conclusions

Spectral evidence coupled with ^{13}C-labeling experiments support a trigonal-bipyramidal (D_{3h}) geometry for $Fe(CO)_3L_2^+$ radicals similar to that of the neutral complexes. Whether the stability of the trigonal-bipyramidal structure arises from steric (*trans*-phosphines), electronic, or solvation effects is unclear; however,

(33) Xiao, S. X.; Trogler, W. C.; Ellis, D. E.; Berkovitch-Yellen, Z. *J. Am. Chem. Soc.* **1983**, *105*, 7033–7037.

Table III. Atomic Character[a] of Frontier Orbitals in $Fe(CO)_3(PH_3)_2^+$: A, D_{3h} Structure; B, C_{2v} Structure

			% contribution from atoms					
orbital	energy, eV[a]	E_{ex}, eV[c]	Fe	orbital charac	C	O	P	H
			Section A					
5e″	−4.02	−0.022	1		9	5	44	41
8e′	−4.83	−0.008	2		5	0	54	39
7e′	−7.16	0.289	24	$d_{x^2-y^2,xy}$	46	28	2	0
4e″	−7.70	0.227	19	$d_{xz,yz}$	47	26	5	3
$4a_2''$	−7.76	0.059	1		47	32	15	5
$2a_2'$	−7.79	0.079	0		63	37	0	0
$6a_1'$	−8.22	0.413	39	d_{z^2}	17	3	30	12
6e′	−11.73[b]	0.460	54	$d_{x^2-y^2,xy}$	26	17	1	3
3e″	−12.71	0.591	77	$d_{xz,yz}$	3	10	4	7
$3a_2''$	−13.80	0.053	2		1	13	79	5
$5a_1'$	−15.15	0.325	46	d_{z^2}	1	0	49	4
5e′	−15.20	−0.011	2		1	2	54	41
2e″	−15.27	−0.001	2		0	8	53	37
$1a_2'$	−16.86	0.080	0		25	75	0	0
4e′	−16.98	0.087	0		33	66	1	0
$2a_2''$	−17.23	0.073	0		32	61	4	2
1e″	−17.29	0.092	3		34	60	2	0
3e′	−17.33	0.210	17	$d_{x^2-y^2,xy}$	32	51	0	0

		% contribution from atoms							
orbital	energy, eV	Fe	orbital charac	C_A[d]	O_A[d]	C_E[e]	O_E[e]	P	H
			Section B						
$9b_2$	−4.96	2		7	3	3	2	45	38
$14a_1$	−5.43	5		4	1	2	0	51	37
$9b_1$	−7.02	12		11	4	41	29	2	0
$13a_1$	−7.20	29		11	2	31	23	3	2
$4a_2$	−7.32	23		0	0	44	25	4	3
$8b_1$	−7.57	19		44	29	7	2	0	0
$8b_2$	−7.66	18		42	25	2	1	9	3
$12a_1$	−7.68	33	$d_{x^2-y^2},d_{z^2}$	2	0	26	8	21	10
$7b_2$	−7.92	2		2	1	47	30	14	4
$11a_1$	−10.04[b]	45	$d_{x^2-y^2},d_{z^2}$	4	2	26	13	8	3
$6b_2$	−12.21	78	d_{yz}	4	9	0	0	3	6
$3a_2$	−12.69	74	d_{xy}	0	0	3	14	3	6
$7b_1$	−12.73	72	d_{xz}	3	7	4	14	0	0
$5b_2$	−13.43	4		0	2	1	9	78	5
$10a_1$	−14.73	34	$d_{x^2-y^2},d_{z^2}$	1	0	0	1	55	10
$9a_1$	−15.22	7		1	0	0	1	53	37
$4b_2$	−15.24	1		0	5	0	0	55	38
$6b_1$	−15.53	0		0	1	24	8	32	34
$2a_2$	−16.80	0		0	0	3	22	39	36
$8a_1$	−16.54	2		5	2	24	67	1	0
$5b_1$	−16.59	0		3	21	27	24	14	10
$4b_1$	−16.66	2		1	2	29	59	4	2
$3b_2$	−16.81	0		2	5	28	62	2	1
$1a_2$	−17.20	4		0	0	34	45	11	5
$2b_2$	−17.21	1		32	58	1	3	3	1
$7a_1$	−17.37	14	$d_{x^2-y^2},d_{z^2}$	28	43	6	8	1	0

[a] From spin-restricted calculations. [b] Denotes highest occupied orbital. [c] Exchange splitting from the spin-polarized calculation. [d] Denotes apical carbon and oxygen. [e] Denotes the two carbons and oxygens that lie in the equatorial plane.

from the spectral parameters of Table I it seems that even the unhindered PMe_3 derivative adopts a similar structure. Molecular orbital calculations show that the intense colors of these radicals arise from transitions within the d–d manifold created by the presence of a hole in the highest lying d orbital. The $Fe(CO)_3L_2^+$ species are known[19] to transfer electrons via an outer-sphere pathway to form Fe(O) and Fe(II) species. The SCF–Xα–DV calculations (Table IV) predict that most of the unpaired electron spin density resides on the metal atom. In contrast, SCF–Xα–DV calculations for $V(CO)_6$,[21] a metal radical thought to transfer electrons by an inner-sphere pathway,[9,10] predict that the vanadium center is highly charged (+1.42) and that considerable unpaired spin and electron density localizes onto the carbonyl ligands. The oxygen atom of bound CO is believed[10] to act as a ligand[34] in an inner-sphere electron-transfer disproportionation reaction for $V(CO)_6$.

The EPR studies of $Mn(CO)_5$ doped into $Cr(CO)_6$ single crystals,[25a] IR spectra of ^{13}CO-labeled $Mn(CO)_5$ in a CO matrix,[25c] and ESR spectra of $Mn(CO)_5$ in krypton[25d] and argon[25e] matrices, providing overwhelming evidence that the solid-state struture of $Mn(CO)_5$ is C_{4v}. Preliminary EPR spectra have also been taken to indicate[14e] a square-pyramidal structure for $Mn(CO)_3L_2$ radicals. Examination of IR and electronic absorption spectral data for $Mn(CO)_3L_2$ compounds leads us to make the following obserations: (1) infrared data reported[14b] for $Mn(CO)_3L_2$ (L = alkylphosphine) complexes show a single CO absorption with a shoulder; (2) electronic spectra of $Mn(CO)_3L_2$ complexes and the electronic spectrum of $Fe(CO)_3(PCy_3)_2^+$ are virtually identical, having intense absorptions at 700 and 1150 nm. It would be desirable to perform ^{13}CO-labeling studies for the substituted Mn radicals to see whether it supports the proposed square-pyramidal structure.

Experimental Section

Materials. The $Fe(CO)_3L_2$ complexes were prepared photochemically from $Fe(CO)_5$ and the appropriate phosphine.[35] Iron pentacarbonyl

(34) Osborne, J. H.; Rheingold, A. L.; Trogler, W. C. *J. Am. Chem. Soc.* **1985**, *107*, 6292–6297.

(35) Therien, M. J.; Trogler, W. C., submitted for publication in Inorg. Syntheses.

Table IV. Calculated[a] Spin Distribution and Orbital Populations in $Fe(CO)_3(PH_3)_2^+$, D_{3h} Structure

atom	orbital	occupation	spin density
Fe	3d	6.65	0.720
	4s	0.09	0.11
	4p	0.54	0.011
		+0.72 pop chg	
		+0.47 $\int_{chg}$	
C	2s	1.32	0.01
	2p	1.55	0.01
		+0.13 pop chg	
		+0.07 $\int_{chg}$	
O	2s	1.83	0.00
	2p	4.50	0.05
		−0.33 pop chg	
		−0.27 $\int_{chg}$	
P	3s	1.53	−0.01
	3p	3.24	−0.03
	3d	0.33	0.00
		+0.1 pop chg	
		+2.14[c] $\int_{chg}$	
H	1s	0.82	0.01
		+0.18 pop chg	
		−0.53[c] $\int_{chg}$	

[a] From spin-polarized calculations. [b] $\int_{chg}$ denotes the charge calculated by volume integration about each atom. [c] The positive charge on P and negative charge on exterior H result from the large region of space-assigned exterior hydrogens (c.f.: Holland, G. F.; Ellis, D. E.; Trogler, W. C. *J. Am. Chem. Soc.* **1986**, *108*, 1884.

Table V. Calculated Dipole-Allowed Transition Energies[a] (A) for D_{3h} $Fe(CO)_3(PH_3)_2^+$ and Observed Electronic Transitions in $Fe(CO)_3(PCy_3)_2^+$ and (B) for C_{2v} $Fe(CO)_3(PH_3)_2^+$

1-e transition	transition type	state symm	calcd energy, eV	exptl energy, eV
		Section A		
$3e'' \rightarrow 6e'$	d → d	$^2E' \rightarrow {}^2E''$	1.06	1.16
$5a_1' \rightarrow 6e'$	Fe–P σ → d	$^2E' \rightarrow {}^2A_1'$	3.71	1.89
$5e' \rightarrow 6e'$	PH_3 → d C.T.	$^2E' \rightarrow {}^2E'$	4.42	4.9
$6e' \rightarrow 6a_1'$	d → Fe–P σ*	$^2E' \rightarrow {}^2A_1', {}^2E', {}^2A_2'$	3.76	3.8
$6e' \rightarrow 4e''$	d → CO π*	$^2E' \rightarrow 2^2E''$	4.14	3.8
$6e' \rightarrow 7e'$	d → CO π*	$^2E' \rightarrow 3^2E', {}^2A_1', {}^2A_2'$	4.67	4.9
		Section B		
$6b_2 \rightarrow 11a_1$	d → Fe–C π	$^2A_1 \rightarrow {}^2B_2$	2.30	
$3a_2 \rightarrow 11a_1$	d → Fe–C π	$^2A_1 \rightarrow {}^2A_2$	2.70	
$7b_1 \rightarrow 11a_1$	d → Fe–C π	$^2A_1 \rightarrow {}^2B_1$	2.76	
$5b_2 \rightarrow 11a_1$	P → Fe–C π	$^2A_1 \rightarrow {}^2B_2$	3.81	
$10a_1 \rightarrow 11a_1$	Fe–Pσ → Fe–C π	$^2A_1 \rightarrow {}^2A_1$	4.95	
$11a_1 \rightarrow 7b_2$	Fe–C π → CO π*	$^2A_1 \rightarrow {}^2B_2$	2.35	
$11a_1 \rightarrow 12a_1$	Fe–C π → Fe–P σ*	$^2A_1 \rightarrow {}^2A_1$	2.46	
$11a_1 \rightarrow 8b_2$	Fe–C π → Fe–C π*	$^2A_1 \rightarrow {}^2B_2$	3.15	

[a] From spin-restricted transition-state calculations.

(Strem), tri-*n*-butylphosphine (Aldrich), tricyclohexylphosphine (Strem), and triphenylphosphine (Strem) were used as received. Trimethylphosphine was synthesized from methylmagnesium iodide and triphenylphosphite and redistilled twice. The $Fe(CO)_3L_2^+$ species were synthesized by a published procedure.[20] Solvents were distilled under an N_2 atmosphere; methylene chloride was refluxed over CaH_2 for 36 h and hydrocarbons (hexanes, cyclohexane) were distilled from sodium benzophenone ketyl. All materials were handled by using standard Schlenk techniques. Manipulations of isolated iron(I) complexes were performed under N_2 in a Vacuum Atmospheres glovebox equipped with an HE-493 Dri-Train. Care was taken to avoid contamination by water and oxygen in all experiments. Since the iron(I) compounds are photosensitive, experimental work was conducted in subdued light.

Labeling Studies. Preparation of 50% ^{13}C-labeled $Fe(CO)_5$ followed a method similar to one in the literature.[36] To 0.5 mL of $Fe(CO)_5$ (3.73 × 10^{-3} mol) in 100 mL of cyclohexane was added 0.80 g of 10% Pd on activated charcoal (Aldrich), a CO-exchange catalyst. The solution was frozen at liquid nitrogen temperature, and the Schlenk flask was evacuated. About 100 mL of ^{13}CO (99.5 atom % Merk, Sharp & Dome) was added at ~0.9 atm, and the vessel was allowed to warm to room temperature. The flask was shaken over a period of several minutes with aliquots removed periodically for IR analysis to determine the extent of ^{13}CO incorporation. The enrichment step was repeated (ca. three exchanges) until the IR spectrum of sampled aliquots matched published spectra[37] for 50% ^{13}CO-labeled $Fe(CO)_5$. The solution was cannula filtered and then used to synthesize 50% ^{13}CO-labeled $Fe(^*CO)_3(PPh_3)_2$. This material was isolated, and synthesis of the corresponding 17-electron complex was performed in the usual manner. A 0.1-mL sample of $Fe(CO)_5$ enriched to 93% with ^{13}CO was prepared by repeating the enrichment step 4–5 times.

Spectral Studies. Infrared spectra were recorded with an IBM FTIR/32 instrument. Electronic absorption spectra were measured with an IBM 9420 UV–vis spectrophotometer equipped with a thermostated cell holder and interfaced to an IBM 9000 computer. Absorption spectra in the near-IR region were obtained with a Cary 17D spectrometer. Quartz cells of 1.0-cm path length, equipped with a ground glass joint and Teflon needle valve, were used to maintain oxygen- and water-free samples. EPR spectra were recorded at room temperature and at 77 K with a Varian E-3 spectrometer that was interfaced to an IBM 9000 computer. External diphenylpicrylhydrazyl was used as the field marker.

Theoretical Studies. Electronic structure calculations were performed with a DEC-VAX 11/750 minicomputer using the self-consistent field discrete variational Xα method (SCF–Xα-DV).[28] Numerical atomic orbitals from exact Hartree–Fock–Slater calculations were used as basis functions, assuming the α values of Schwartz.[38] For Fe the atomic orbitals through 4p were included, for P, the atomic orbitals through 3d were used as a basis, for C and O, a minimal 1s, 2s, 2p basis was used, and for H a 1s function was used. Core orbitals (1s, ..., 3p for Fe, 1s, 2s,2p for P, and 1s for C and O) were frozen and orthogonalized against valence orbitals. The Mulliken[39] scheme was used to compute atomic orbital populations. The molecular Coulomb potential was calculated by using a least-squares fit[28] of the model electron density to the true density. Seven radial degrees of freedom were allowed in the expansion of the density, in addition to the radial atomic densities. For the molecular exchange potential $\alpha = 0.71151$. Spin-restricted and spin-polarized[40] SCF–Xα–DV calculations were performed to deduce qualitative bonding features. Transition-state studies employed spin-restricted SCF–Xα–DV calculations to estimate the energies of the dipole-allowed electronic transitions. As a computationally accessible model for the 17-electron $Fe(CO)_3(PR_3)_2^+$ complexes we used $Fe(CO)_3(PH_3)_2^+$, the structure of which was idealized to D_{3h}, C_s, and C_{2v} symmetries. The assumed bond length to hydrogen atoms that replaced the alkyl or aryl groups bound to phosphorus was 1.415 Å. The Fe–C, C–O, and Fe–P bond distances were taken to be 1.758, 1.156, and 2.213 Å, respectively, from published[32] X-ray data. For the C_{2v} and C_s models, the L_{basal}–Fe–L_{basal} and L_{basal}–Fe–CO_{basal} angles, respectively, were chosen to be 172° as predicted for d^7 ML_5 complexes by extended Hückel calculations.[26a]

Acknowledgment. This material is based on work supported by the National Science Foundation (Grant CHE-85-04088). We thank Prof. R. N. Perutz and Prof. T. L. Brown for helpful discussions and Dr. J. H. Osborne for computational and experimental assistance. W.C.T. thanks the Alfred P. Sloan Foundation for a research fellowship.

Registry No. $Fe(CO)_3(PPh_3)_2$, 21255-52-7; $[Fe(CO)_3(PPh_3)_2][PF_6]$, 73979-30-3; $Fe(CO)_3(PMe_3)_2^+$, 102133-38-0; $Fe(CO)_3(P(n\text{-}Bu)_3)_2^+$, 102133-39-1; $Fe(CO)_3(P(c\text{-}C_6H_{11})_3)_2^+$, 102133-40-4; $[Fe(CO)_3(P(c\text{-}C_6H_{11})_3)_2][PF_6]$, 102133-41-5.

Supplementary Material Available: Tables of orbital energies and transition-state calculations for the C_s square-pyramidal isomer of $Fe(CO)_3(PH_3)_2^+$ with cis equatorial phosphines (2 pages). Ordering information is given on any current masthead page.

(36) Noak, K.; Ruch, M. *J. Organomet. Chem.* **1984**, *17*, 309–322.
(37) Mahnke, H.; Sheline, R. K. *Inorg. Chem.* **1976**, *5*, 1245–1246.
(38) Schwartz, K. *Phys. Rev.B: Solid State* **1972**, *5*, 2466–2468.
(39) Mulliken, R. S. *J. Chem. Phys.* **1955**, *23*, 1833–1840.
(40) Delley, B.; Ellis, D. E.; Freeman, A. J.; Barends, E. J.; Post, D. *Phys. Rev. B: Solid State* **1983**, *27*, 2132–2144.